PHYSICAL REVIEW B VOLUME 57, NUMBER 11 15 MARCH 1998-I

Resistivity determination from small crystallites

S. Hyun, M. F. Thorpe, M. D. Jaeger, and B. Golding
Department of Physics & Astronomy, and Center for Sensor Materials, Michigan State University, East Lansing, Michigan 48824

A. R. Day
Department of Physics, Marquette University, Milwaukee, Wisconsin 53233

(Received 11 July 1997)

We determine the resistivity of small micrometer-sized conductors with arbitrary shapes. It is shown that with n terminals attached to the sample, there are $n(n-1)/2$ *independent* measurements of the resistance that can be made; from which the sample resistivity and the contact resistances can be extracted. An image of the sample is digitized and a finite element analysis is used to determine the geometrical factors that arise from the nonuniform current flow and hence control the resistance measurements. It is shown that all the elements of the resistance matrix for the sample are generated from the diagonal elements alone for an Ohmic sample, which provide a useful check of the experimental resistance measurements. To illustrate this approach, micrometer-sized diamond crystallites with four terminals were used, and the sample resistivity and the contact resistances extracted. This technique is a practical example of an inverse problem. [S0163-1829(98)02211-5]

I. INTRODUCTION

The determination of the resistivity of a regularly shaped macroscopic sample is usually straightforward, both in principle and in practice. For a suitable choice of the sample geometry there is a region where the current flow is uniform and, if the voltage is sampled across this region the measurements are independent of the contact resistances [a so-called four-terminal measurement] and the resistivity is easily obtained. An example of this is a rectangular bar with current contacts near both ends and voltage probes near the center of the bar. However, this approach is not possible for many samples for which regular shapes are difficult to obtain or fabricate, but which may nevertheless be of considerable interest. As an example, consider a single crystal of an electrically isotropic material from which it is desired to determine the absolute value of its resistivity as well as its temperature dependence.

This technique should be regarded as a *material properties inverse problem* following Kubo's classification.[1] The term *inverse problem* can be defined simply as the determination of the *causes* from the *results*. It is opposite to the *direct problem* that determines the *results* from given *causes*. Let ϕ be a field variable representing a physical state of the system, which is a response to an applied force f. Then a governing equation can be written as

$$L(k)\phi=f, \tag{1}$$

where $L(k)$ is an operator and k denotes material properties of the system. The inverse problem is, given the response ϕ and the applied force f, to determine any missing information involving geometry, operator form, boundary conditions, and material properties in Eq. (1).

In this paper we present a new method to determine the resistivity of any arbitrarily shaped three-dimensional object that is known *a priori* to have isotropic electrical properties. In this problem, the applied force of Eq. (1) is the current and the response is the potential. We know the form of the operator L and the material property we wish to determine is the resistivity. Specifically, the I-V characteristics of the crystallite can be viewed as *results* and we identify the resistivity and contact resistances as *causes*. In the process of accomplishing this, we also show how *all* the individual contact resistances can be found as a byproduct of our analysis. We demonstrate this technique by measurements on micrometer-sized single crystals of doped, semiconducting diamond.[2]

The diamond crystallites in this study were grown by a chemical vapor deposition (CVD) technique on a silicon substrate. Au/Ti contact pads were attached to the samples and gold leads for the current and voltage probes were attached to the pads. The details of the experimental technique are described in Ref. 2. An electron micrograph of one of the two samples analyzed in this paper is shown in Fig. 1. It is a well-faceted, single crystal of micrometer-sized diamond. Since the current flow pattern is complicated in such an arbitrarily shaped sample, it is not possible to extract the sample resistivity in any simple way. It is the resistivity, which is a material property and hence independent of the sample shape, that is of the most interest in characterizing the sample. Although there is a well-known four-probe method to determine the resistivity, as first suggested by van der Pauw,[3] it is only valid for a quasi-two-dimensional sample and there is also a restriction that the contacts be points on the sample perimeter.[4]

In the next section we discuss some general constraints on the resistance measurements. In Sec. III we describe how to set up a finite element representation of the sample and use it to determine the sample resistivity from resistance measurements. In Sec. IV we apply this method to data taken on two samples and discuss the results. In Sec. V we summarize our results and the application of the method.

II. RESISTANCE TABLE AND RECIPROCITY THEOREM

A sample with n terminals attached can be described by an equivalent electrical circuit of ${}^nC_2$ resistors connecting

 © 1998 The American Physical Society

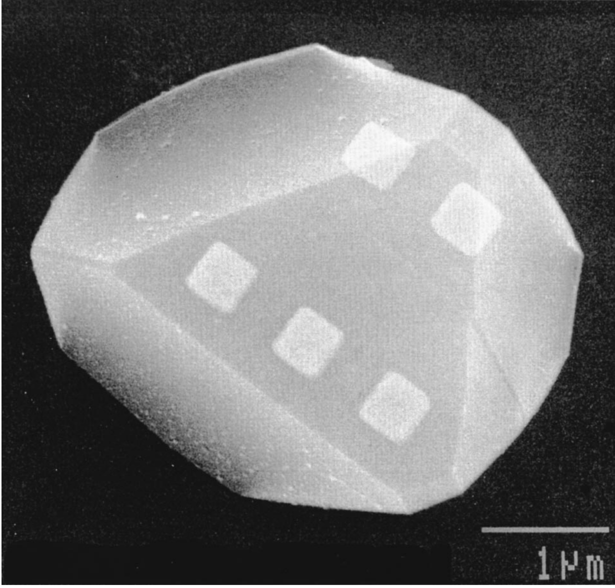

FIG. 1. Micrometer-sized diamond crystallite grown by a chemical vapor deposition technique. Diamond crystallite (sample 2) with contact pads prior to lithographic lead attachment. Four of the five pads were used for the measurement, with the furthest to the left having no lead attached. This pad was at a constant potential that was determined by the finite element code.

each pair of terminals. Measurements are done by injecting a current I_{lm} in at terminal l and out at terminal m, and then measuring a potential difference V_{ij} across terminals i and j. We can define a (signed) resistance $R^{ij}_{lm}=V_{ij}/I_{lm}$, which reduces to the standard definition of resistance when $i,j=l,m$. This set of measurements forms a ${}^{n}C_2$ by ${}^{n}C_2$ resistance matrix of all possible pairs of current terminals and voltage terminals but there are only ${}^{n}C_2$ independent elements in this matrix because of the following constraints:

(1) For an Ohmic sample, the matrix is symmetric under exchange of current and voltage terminals, i.e.,

$$R^{ij}_{lm}=\frac{V_{ij}}{I_{lm}}=R^{lm}_{ij}=\frac{V_{lm}}{I_{ij}}, \tag{2}$$

where V_{ij} is the voltage between the leads i, j, and I_{lm} is the current between the leads l, m. This is a *reciprocity theorem*,[5,6] which is proved in the Appendix for the present geometry. (2) Along any row of the resistance matrix the current is a constant, and the voltage is a scalar potential, that satisfies

$$V_{ij}=V_{ik}+V_{kj}. \tag{3}$$

Thus, the resistance elements have the additive property

$$R^{ij}_{lm}=R^{ik}_{lm}+R^{kj}_{lm}. \tag{4}$$

Using these two rules we can show that there are only ${}^{n}C_2$ independent elements in the resistance matrix by the following construction:

Consider the $n-1$ elements ($R^{1i}_{12}, i=2,\ldots,n$) in the first row of the resistance matrix. These terms can generate all the other elements in this row using the addition rule,

TABLE I. Showing the number of independent elements in the resistance table. We need at least four terminals to extract the resistivity ρ and the contact resistances because otherwise there are more unknowns than independent terms.

Number of terminal	Dimension of resistance table	Elements in resistance table	Number of independent elements	Unknowns (ρ, contact resistances)
2	1	1	1	3
3	3	9	3	4
4	6	36	6	5
5	10	100	10	6
6	15	225	15	7
n	${}^{n}C_2=\frac{n(n-1)}{2}$	$[{}^{n}C_2]^2$	${}^{n}C_2=\frac{n(n-1)}{2}$	$n+1$

$$R^{ij}_{12}=R^{1j}_{12}-R^{1i}_{12}, \tag{5}$$

where $i<j=2,\ldots n$. Note that changing the order of the indices changes the sign of the resistance. In the second row, only $n-2$ elements of R^{li}_{13} ($i=3,\ldots n$) are needed to construct the remaining elements in that row because, by the reciprocity theorem, $R^{12}_{13}=R^{13}_{12}$ and R^{13}_{12} was given in the first row. Continuing in this manner we need $n-1$ terms in the first row, $n-2$ terms in the second row etc., for a total of

$$(n-1)+(n-2)+\cdots+2+1=\frac{n(n-1)}{2}={}^{n}C_2 \tag{6}$$

independent elements. There are many possible choices of the ${}^{n}C_2$ independent elements, but they cannot be selected arbitrarily. Surprisingly, the ${}^{n}C_2$ diagonal elements (the set of 2 terminal elements) also form an independent set, related to the off diagonal elements by

$$R^{lm}_{ij}=\frac{R^{jl}_{jl}+R^{im}_{im}-R^{jm}_{jm}-R^{il}_{il}}{2}. \tag{7}$$

This relation (7) means that a knowledge of only the two terminal measurements can be used to generate the complete resistance matrix, which can be used as a useful self-consistency check on the experimental results. It is also interesting to note that the set of four terminal measurements are not all independent. Table I shows how the number of elements in the resistance matrix and the number of independent elements depend on the number of terminals.

As an example, consider the case for $n=4$ terminals shown in Fig. 2. There are six ways to select two of four terminals and so there is a 6×6 resistance matrix with six independent elements. The six diagonal elements form the most important set of independent elements from which we can use Eq. (7) to obtain the three off-diagonal terms, R^{13}_{12}, R^{14}_{12}, R^{14}_{13}, as shown in Table II. The 3×3 upper diagonal block [shown inside the bold line in Table II] is an alternative independent set that can be used to construct the entire matrix using the procedure outlined above. Note that by Eq. (7), only two of the four terminal elements are independent with

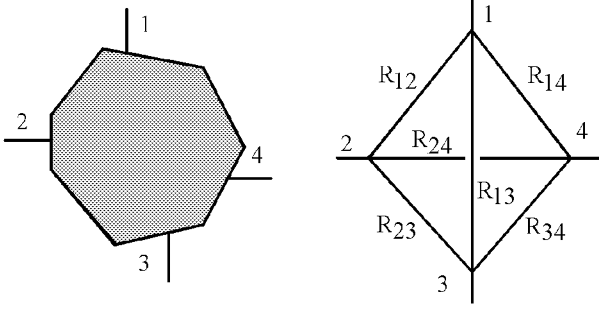

FIG. 2. Equivalent circuit for a sample with four terminals. The number of resistors is ${}^{n}C_2$ for a sample with n contacts.

$$R_{13}^{24}=R_{14}^{23}+R_{12}^{34}. \tag{8}$$

As a result, a set of six terms including three four-terminal measurements *cannot* be used to reconstruct the whole resistance table.

It is important to note that the above analysis is only true for samples where the I-V curve is independent of the current direction (otherwise the reciprocity theorem fails). Some of the experimental data analyzed in Sec. IV has non-Ohmic characteristics, and so the resistance matrix has more than six independent elements. The necessary modifications to the above analysis are model dependent, and will be discussed for the specific situation of the experiment.

III. COMPUTER SIMULATION

We formed a three dimensional computer model of the small crystal from scanning electron microscope (SEM) pictures taken along several different orientations.[2] An *inverse* ray tracing technique was used to reconstruct the three-dimensional object from a set of two-dimensional pictures. Ray tracing is a computer process used to create a two-dimensional representation of a three-dimensional object by tracing the path of the ray of light between the light source, objects, and an observer.[7] We apply this technique in *reverse* to construct a three-dimensional image from the two-dimensional SEM pictures.

The algorithm treats the crystal as an irregular polyhedron and attempts to assign coordinates to the vertices in a way that is consistent with the SEM images. From each picture of the crystal we can measure the *projected* length of an edge of the diamond crystal, and compare it with the projected length calculated from the assumed vertex coordinates. The vertex coordinates are adjusted to try to minimize

$$\chi_l^2=\sum_i\left[\frac{l_i-l_i^{\mathrm{SEM}}}{\sigma_i^l}\right]^2, \tag{9}$$

where l_i is a calculated projected length, l_i^{SEM} is the projected length from the SEM and σ_i is an estimate of the experimental error in measuring l_i^{SEM}. The sum is over all edges visible in each picture, and over all pictures. The positions of the contact pads are determined by including the coordinates of the corners of the contact pads, and the lengths from the corners to some of the crystal vertices. Taking pictures from enough different orientations to ensure that every edge was visible in at least two images was adequate to ensure that we could construct a representation of the sample that matched the SEM images very well. Because we knew that the sample was a single crystal we added some additional constraints to the minimization process. Specifically, we required the facets to be planar, and the facet angles to conform to the known facet angles of the diamond structure, e.g., 70.5° or 109.4° between (111) facets. The flatness constraint was achieved by adding to χ^2 the term

$$\chi_p^2=\sum_i\sum_j\left[\frac{\mathbf{c}_i\cdot(\mathbf{r}_{ij}-\mathbf{c}_i)}{\sigma_i^p}\right]^2, \tag{10}$$

where $\mathbf{r}_{ij}$ denotes jth vertex coordinate in the ith facet and $\mathbf{c}_i$ is a constant vector that is normal to the ith plane. The facet angles are constrained by adding to χ^2 a term

$$\chi_f^2=\sum_i\left[\frac{\theta_i-\theta_i^{\mathrm{theory}}}{\sigma_i^f}\right]^2, \tag{11}$$

where the facet angles $\theta_i^{\mathrm{theory}}$ are those appropriate for a diamond structure. The sum is over pairs of facets. The σ_i^p, σ_i^f in Eqs. (10) and (11) are standard deviations denoting the weighting factors for each constraint. Although it is arbitrary how these factors are assigned they should be larger than the standard deviation associated with the edge lengths l_i because these lengths could be determined very easily and directly from the SEM photographs.

The total χ^2, the sum of the three quantities in Eqs. (9)–(11),

$$\chi^2=\chi_l^2+\chi_p^2+\chi_f^2, \tag{12}$$

TABLE II. A resistance table can be generated from the six terms in the triangular matrix in the bold box by using Eq. (5) and the reciprocity theorm.

R	V_{12}	V_{13}	V_{14}	V_{23}	V_{24}	V_{34}
I_{12}	R_{12}^{12}	$\frac{R_{12}^{12}+R_{13}^{13}-R_{23}^{23}}{2}$	$\frac{R_{12}^{12}+R_{14}^{14}-R_{24}^{24}}{2}$			
I_{13}		R_{13}^{13}	$\frac{R_{13}^{13}+R_{14}^{14}-R_{34}^{34}}{2}$			
I_{14}			R_{14}^{14}			
I_{23}				R_{23}^{23}		
I_{24}					R_{24}^{24}	
I_{34}						R_{34}^{34}

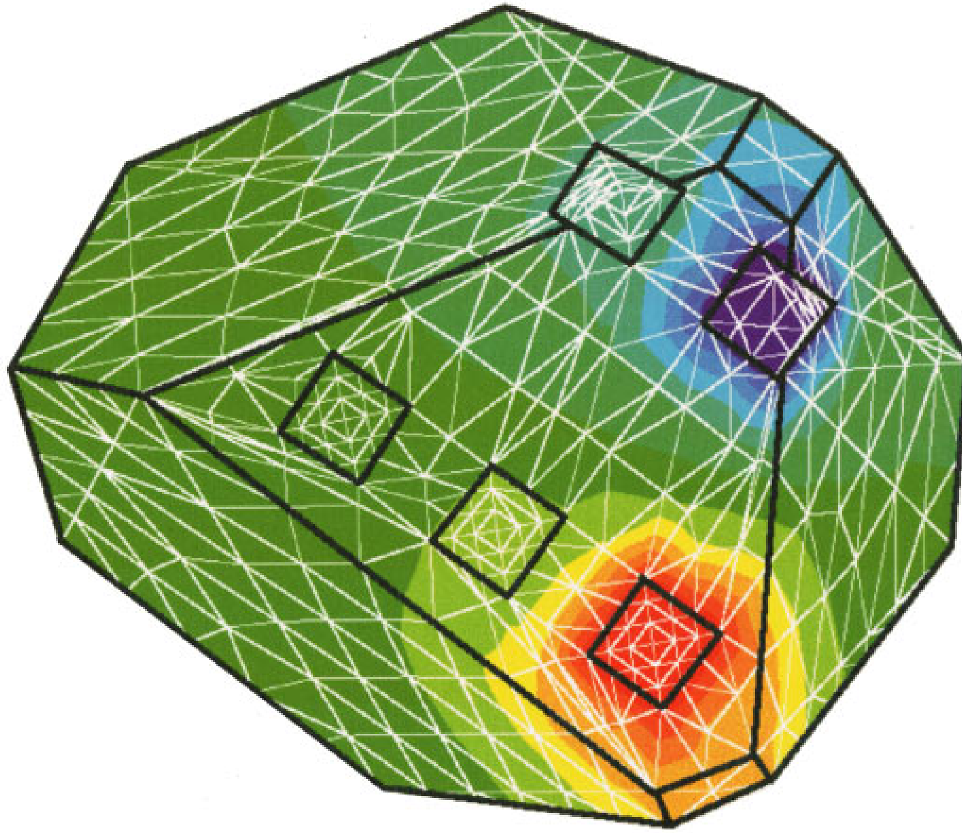

FIG. 3. (Color.) Meshes were generated by ANSYS 6.1 and the equipotential lines given by the finite element simulations using ABAQUS 5.5 are shown on the surface of the sample 2. Current flows from the red pad (high potential) to the blue pad (low potential), as shown by the color scheme.

is minimized by adjusting the vertex coordinates using a standard nonlinear minimization routine.[8] The final coordinates associated with the minimized χ^2 were used as the input for the current flow analysis, which was done using the finite element method (FEM). Figure 3 shows a view of the computer model of the second sample, which can be compared with the SEM image in Fig. 1.

There are three main procedures in the FEM, a preprocessor to generate meshes and set up the initial conditions, an analysis to solve the problem, and a postprocessor to display the results. All FEM tasks in this problem were performed by the commercial packages ANSYS (Ref. 9) and ABAQUS.[10] ANSYS was used for a preprocessor and the other processes (numerical analysis and postprocessor) were done by ABAQUS. From this analysis, a resistance table was obtained by selecting all possible combinations of voltage and current measurements. The contact pads were treated as equipotentials, because of their high conductivity relative to the conductivity of the sample, and the bulk material was assigned a unit resistivity. This leads to a set of *geometrical factors* Γ_{ij}^{lm} (with dimensions of inverse length) for the sample. In the absence of any contact resistances the Γ_{ij}^{lm} are related to the resistances defined in Sec. II by a simple linear relation,

$$R_{ij}^{lm} = \rho \Gamma_{ij}^{lm}, \tag{13}$$

because the resistivity ρ of a single crystal of diamond is isotropic by the crystal symmetry. These geometrical factors

TABLE III. Resistance table with contact resistances r_i, r_1' for current flow in, out of the sample. Another table for reverse current flows is necessary to extract all the contact resistances for non-Ohmic contacts.

R	V_{12}	V_{13}	V_{14}	V_{23}	V_{24}	V_{34}
I_{12}	$R_{12}^{12}+r_1+r_2'$	$R_{12}^{13}+r_1$	$R_{12}^{14}+r_1$	$R_{12}^{23}-r_2'$	$R_{12}^{24}-r_2'$	R_{12}^{34}
I_{13}	$R_{13}^{12}+r_1$	$R_{13}^{13}+r_1+r_3'$	$R_{13}^{14}+r_1$	$R_{13}^{23}+r_3'$	R_{13}^{24}	$R_{13}^{34}-r_3'$
I_{14}	$R_{14}^{12}+r_1$	$R_{14}^{13}+r_1$	$R_{14}^{14}+r_1+r_4'$	R_{14}^{23}	$R_{14}^{24}+r_4'$	$R_{14}^{34}+r_4'$
I_{23}	$R_{23}^{12}-r_2$	$R_{23}^{13}+r_3'$	R_{23}^{14}	$R_{23}^{23}+r_2+r_3'$	$R_{23}^{24}+r_2$	$R_{23}^{34}-r_3'$
I_{24}	$R_{24}^{12}-r_2$	R_{24}^{13}	$R_{24}^{14}+r_4'$	$R_{24}^{23}+r_2$	$R_{24}^{24}+r_2+r_4'$	$R_{24}^{34}+r_4'$
I_{34}	R_{34}^{12}	$R_{34}^{13}-r_3$	$R_{34}^{14}+r_4'$	$R_{34}^{23}-r_3$	$R_{34}^{24}+r_4'$	$R_{34}^{34}+r_3+r_4'$

TABLE IV. The resistance table obtained from an average of Table III and a similar table with all the current and voltage leads reversed.

$\bar{R}$	V_{12}	V_{13}	V_{14}	V_{23}	V_{24}	V_{34}
I_{12}	$R^{12}_{12}+\bar{r}_1+\bar{r}_2$	$R^{13}_{12}+\bar{r}_1$	$R^{14}_{12}+\bar{r}_1$	$R^{23}_{12}-\bar{r}_2$	$R^{24}_{12}-\bar{r}_2$	R^{34}_{12}
I_{13}	$R^{12}_{13}+\bar{r}_1$	$R^{13}_{13}+\bar{r}_1+\bar{r}_3$	$R^{14}_{13}+\bar{r}_1$	$R^{23}_{13}+\bar{r}_3$	R^{24}_{13}	$R^{34}_{13}-\bar{r}_3$
I_{14}	$R^{12}_{14}+\bar{r}_1$	$R^{13}_{14}+\bar{r}_1$	$R^{14}_{14}+\bar{r}_1+\bar{r}_4$	R^{23}_{14}	$R^{24}_{14}+\bar{r}_4$	$R^{34}_{14}+\bar{r}_4$
I_{23}	$R^{12}_{23}-\bar{r}_2$	$R^{13}_{23}+\bar{r}_3$	R^{14}_{23}	$R^{23}_{23}+\bar{r}_2+\bar{r}_3$	$R^{24}_{23}+\bar{r}_2$	$R^{34}_{23}-\bar{r}_3$
I_{24}	$R^{12}_{24}-\bar{r}_2$	R^{13}_{24}	$R^{14}_{24}+\bar{r}_4$	$R^{23}_{24}+\bar{r}_2$	$R^{24}_{24}+\bar{r}_2+\bar{r}_4$	$R^{34}_{24}+\bar{r}_4$
I_{34}	R^{12}_{34}	$R^{13}_{34}-\bar{r}_3$	$R^{14}_{34}+\bar{r}_4$	$R^{23}_{34}-\bar{r}_3$	$R^{24}_{34}+\bar{r}_4$	$R^{34}_{34}+\bar{r}_3+\bar{r}_4$

represent the effects of the nonuniform current flow across the arbitrarily shaped sample. In the absence of contact resistances the experiment measures the resistances R^{lm}_{ij} and with the computed Γ^{lm}_{ij} we can determine ρ.

The measured resistances do include the effect of contact resistances so Eq. (13) must be modified. We assume these contact resistances can be added *in series* to the sample resistance because the contact area is assumed to be an equipotential due to the high conductivity of the Au/Ti contact pads. This leads to

$$R^{lm}_{ij}=\rho\Gamma^{lm}_{ij}+r_i(\delta_{il}-\delta_{im})+r_j(\delta_{jm}-\delta_{jl}). \tag{14}$$

where r_i is the Ohmic contact resistance of terminal i. However, contact resistances are generally non-Ohmic, which is indicated by nonsymmetric three-terminal elements in the observed resistance table. We assume that the sample itself is Ohmic, which is justified if the four-terminal elements are symmetric. Since the I-V characteristics are nonlinear and not symmetric for non-Ohmic behavior of the contacts, each contact has two independent resistances for the two different current directions [i.e., current reversal with the magnitude of the current held constant]. To investigate such non-Ohmic I-V characteristics of a contact, we used two fitting parameters r_i, r'_i corresponding to the two contact resistances for constant current flow. If r_i is a contact resistance when a current is flowing *into* the sample and r'_i is for a current flowing *out* of the sample, then Eq. (14) is modified to become

$$\begin{aligned}R^{lm}_{ij}&=\rho\Gamma^{lm}_{ij}+r_i(\delta_{il}-\delta_{im})+r'_j(\delta_{jm}-\delta_{jl})\\&=\rho\Gamma^{lm}_{ij}+\bar{r}_i(\delta_{il}-\delta_{im})+\bar{r}_j(\delta_{jm}-\delta_{jl})\\&\quad+\Delta r_i(\delta_{il}-\delta_{im})-\Delta r_j(\delta_{jm}-\delta_{jl}),\end{aligned} \tag{15}$$

where

$$\bar{r}_i=\tfrac{1}{2}(r_i+r'_i) \tag{16}$$

and

$$\Delta r_i=\tfrac{1}{2}(r_i-r'_i), \tag{17}$$

which we refer to as the Ohmic and the non-Ohmic parts of the contact resistances, respectively.

Table III is a modified resistance table for a four-terminal problem showing each element in terms of the sample resistivity ρ, the geometric factors Γ^{lm}_{ij} for the sample resistances R^{lm}_{ij} in Eq. (13), and six of the eight contact resistances (r_1, r_2, r'_2, r_3, r'_3, r'_4).[11]

A similar resistance table with both current and voltage leads reversed enables us to construct a resistance table $\bar{R}^{lm}_{ij}=\frac{1}{2}(R^{lm}_{ij}+R^{ml}_{ji})$, which is shown in Table IV, and the $\Delta R^{lm}_{ij}=\frac{1}{2}(R^{lm}_{ij}-R^{ml}_{ji})$, shown in Table V. Throughout this paper we assume that the sample (but not the contacts) are Ohmic. Therefore we have $\bar{R}^{lm}_{ij}=R^{lm}_{ij}=R^{ml}_{ji}$ and $\Delta R^{lm}_{ij}=0$. Note that the resistance Table IV displays all the symmetries of the analysis in Sec. II, and, in particular, only the six diagonal (two-terminal) elements are needed to generate the entire table. For the non-Ohmic resistance table, the six diagonal elements only determine the off-diagonal elements up to an arbitrary constant. To determine all the Δr_i it is necessary to have at least one of the three-terminal elements. For this model, the non-Ohmic resistance table is independent of the resistivity, because we have assumed that the material itself is Ohmic.

Because the geometric factors are known from the FEM we can, in principle, obtain the resistivity and the contact resistances by doing a least-squares fit for the expressions in Tables III–V and the measured resistance; i.e., we minimize a χ^2 defined by

TABLE V. The non-Ohmic resistance table obtained from one half the difference of Table III and a similar table with all the current and voltage leads reversed.

ΔR	V_{12}	V_{13}	V_{14}	V_{23}	V_{24}	V_{34}
I_{12}	$\Delta r_1-\Delta r_2$	Δr_1	Δr_1	Δr_2	Δr_2	0
I_{13}	Δr_1	$\Delta r_1-\Delta r_3$	Δr_1	$-\Delta r_3$	0	Δr_3
I_{14}	Δr_1	Δr_1	$\Delta r_1-\Delta r_4$	0	$-\Delta r_4$	$-\Delta r_4$
I_{23}	$-\Delta r_2$	$-\Delta r_3$	0	$\Delta r_2-\Delta r_3$	Δr_2	Δr_3
I_{24}	$-\Delta r_2$	0	$-\Delta r_4$	Δr_2	$\Delta r_2-\Delta r_4$	$-\Delta r_4$
I_{34}	0	$-\Delta r_3$	$-\Delta r_4$	$-\Delta r_3$	$-\Delta r_4$	$\Delta r_3-\Delta r_4$

TABLE VI. Resistances obtained from the experimental measurement for sample 1 (in kΩ). Diagonal terms in boldface denote two-terminal measurements and the underlined values are four-terminal measurements.

R	V_{12}	V_{13}	V_{14}	V_{23}	V_{24}	V_{34}
I_{12}	**720.0**	560.0	508.0	−176.0	−231.8	−55.5
I_{13}	568.7	**1039.0**	534.5	497.3	−34.7	−531.1
I_{14}	518.4	540.2	**986.0**	20.2	500.0	476.9
I_{23}	−174.5	498.7	20.7	**665.0**	195.1	−477.7
I_{24}	−230.6	−35.2	498.5	195.4	**718.0**	531.0
I_{34}	−55.7	−534.2	473.7	−477.6	529.2	**999.0**

TABLE VII. Geometrical factors from the finite element method for sample 1 (in μm^{-1}). Diagonal terms in boldface denote two-terminal measurements and the underlined values are four-terminal measurements.

Γ	V_{12}	V_{13}	V_{14}	V_{23}	V_{24}	V_{34}
I_{12}	**1.6609**	0.9635	0.7955	−0.6974	−0.8653	0.1679
I_{13}	0.9634	**1.9550**	0.9568	0.9916	−0.006647	−0.9982
I_{14}	0.7957	0.9569	**1.5608**	0.1612	0.7651	0.6039
I_{23}	−0.6973	0.9916	0.1613	**1.6889**	0.8586	−0.8303
I_{24}	−0.8652	−0.006684	0.7651	0.8585	**1.6303**	0.7718
I_{34}	−0.1679	−0.9982	0.6038	−0.8303	0.7717	**1.6021**

TABLE VIII. Resistivity and contact resistances for sample 1, *assuming* that all the contact resistances were Ohmic. (a) The resistivity was fitted by six four-terminal measurements and contacts were given by whole elements. (b) All parameters were fitted by six diagonal terms. (c) With the resistivity from four-terminal measurements, contacts were fitted by diagonal terms. (d) All parameters were given by whole elements.

	ρ (Ω cm)	r_1 (kΩ)	r_2 (kΩ)	r_3 (kΩ)	r_4 (kΩ)
(a)	23.72	316.3	6.1	276.2	329.0
(b)	22.50	314.0	15.0	285.0	336.0
(c)	23.72	303.3	5.6	274.0	329.0
(d)	23.58	317.6	7.3	277.5	330.0

TABLE IX. Resistances obtained from the experimental measurement for sample 2 (in kΩ). All measurement were done at constant current (100 nA) at room temperature ($T=20\ ^\circ C$). The values in parenthesis in the diagonal terms are measured for a reversed current flow. The different magnitudes in these two measurements show the non-Ohmic behavior of the contacts. Diagonal terms in boldface denote two-terminal measurements and the underlined values are four-terminal measurements.

R	V_{12}	V_{13}	V_{14}	V_{23}	V_{24}	V_{34}
I_{12}	**875 (875)**	386	369	−432.3	−451	−18.1
I_{13}	392	**3771 (4878)**	587	3240	203	−3032
I_{14}	369.5	389	**1591 (1591)**	212	1114	917
I_{23}	−450	3255	221	**3774 (4936)**	663	−3026
I_{24}	−471	192	1126	654	**1705 (1705)**	943
I_{34}	−20.1	−4207	918.9	−4190	935	**5236 (4098)**

TABLE X. Geometrical factors from the finite element method for sample 2 (in $\mu\mathrm{m}^{-1}$). Diagonal terms in boldface denote two-terminal measurements and the underlined values are four-terminal measurements.

Γ	V_{12}	V_{13}	V_{14}	V_{23}	V_{24}	V_{34}
I_{12}	**1.0825**	0.6336	0.6049	−0.4489	−0.4777	$\underline{-0.02869}$
I_{13}	0.6336	**1.4178**	0.9440	0.7843	$\underline{0.3104}$	−0.4737
I_{14}	0.6049	0.9440	**1.4112**	$\underline{0.3391}$	0.8064	0.4671
I_{23}	−0.4489	0.7842	$\underline{0.3391}$	**1.2332**	0.7880	−0.4450
I_{24}	−0.4776	$\underline{0.3104}$	0.8064	0.7880	**1.2840**	0.4958
I_{34}	$\underline{-0.02869}$	−0.4738	0.4673	−0.4452	0.4960	**0.9407**

$$\chi^2=\sum_i \left[\frac{R_i^e-R_i^t(\rho,r)}{\sigma_i}\right]^2, \tag{18}$$

where R_i^e are the experimental measurements and $R_i^t(\rho,r)$ are the theoretical resistances defined by Eq. (15) as a function of the resistivity ρ and contact resistances r. The sum is over the elements of the resistance matrix used for fitting and σ_i is a standard deviation of each experimental measurement, which includes both errors in the resistance measurements, and errors in the geometric factors caused by the errors in the computer model of the crystallite, and the FEM. In practice, the least-squares fit is best done separately for the Ohmic and the non-Ohmic parts (Tables IV and V). The practical details of this fitting will be discussed in the next section, when it is applied to our two samples.

IV. RESULTS

As an illustration of this technique, we used two diamond crystallites with four terminals. (see Fig. 1) A resistance matrix for sample 1 (Table VI) was completed by making all 36 resistance measurements. A 6×6 matrix of geometrical factors is obtained by using the FEM and shown in Table VII. Within the experimental error, Table VI is symmetric, which indicates that r_2 and r_3 are Ohmic. If the contact resistances are Ohmic, we can determine the resistivity ρ and the four contact resistances ($r_i=r_i'=\bar{r}_i, i=1,4$). As a check of the validity of applying the analysis of Sec. II, we first calculated the resistivity from the four-terminal measurements (where $R_{ij}^{lm}=\rho\Gamma_{ij}^{lm}$) with a linear fit through all six data points and the origin. We then used this ρ to determine the contact resistances from the three-terminal measurements (each of which involves only one contact resistance) and then averaged the results. The results are shown in row (a) of Table VIII. We then used Eq. (14) to do a least-squares fit for five parameters to the six two-terminal measurements. The results are shown in row (b) of Table VIII. In row (c) of Table VIII, the resistivity was fitted by four-terminal measurements as in (a), and four contact resistances were obtained from six diagonal terms by a least-squares fit. Finally, we fitted five parameters with all 36 elements of the resistance matrix, the results of which are shown in row (d) of Table VIII. It is clear that all four methods give essentially the same results. Note that one of the contacts has a very small resistance compared to the others.

The measured resistance matrix for sample 2 (as shown in Fig. 1) is given in Table IX. Using Table III, it is clear from the asymmetries that contact resistance 3 was very non-Ohmic, and that contact resistance 2 has a small non-Ohmic part. As discussed in the previous section, a second set of measurements should be taken, with the current and voltage probes reversed. This was only done for the six diagonal (two-terminal) elements before the leads were damaged. Nevertheless, this is a sufficient set of data to determine the resistivity and all the contact resistances. The reversed current measurements are shown in parentheses in the table.

The geometrical factors for sample 2 are given in Table X. We processed the data for sample 2 in four distinct ways to test the accuracy of the fitting procedure. In the first method we first calculated the resistivity from the four-terminal measurements and with this ρ determined six of the eight contact resistances from the three-terminal measurements, and the remaining two contact resistances (r_1' and r_4) from the diagonal elements with the currents reversed. These results are shown in row (a) of Table XI. In the second method we did a least-squares fit to obtain the resistivity and the Ohmic part of the contact resistances ($\bar{r}_i$, $i=1,4$), from the six diagonal elements of $\bar{R}_{ij}^{lm}$. From the six diagonal elements of ΔR_{ij}^{lm}, and the three-terminal elements of the

TABLE XI. Resistivity and contact resistances for sample 2. The small negative resistances are not real and result from the small resistance of pad 1 compared to the other three pads. (a) The resistivity was fitted by four-terminal measurements and contacts were given by whole elements. (b) The resistivity and $\bar{r}_i$ were given by $\bar{R}_{ij}^{lm}$. And Δr_i were fitted by ΔR_{ij}^{lm} with Δr_2 given by three-terminal terms in Table IX. (c) Using the resistivity given by four-terminal measurements, $\bar{r}_i$ were obtained by $\bar{R}_{ij}^{lm}$, and Δr_i are same with (b). (d) All of parameters were fitted by using all the elements.

	ρ (Ω cm)	$\bar{r}_1,\Delta r_1$ (kΩ)	$\bar{r}_2,\Delta r_2$ (kΩ)	$\bar{r}_3,\Delta r_3$ (kΩ)	$\bar{r}_4,\Delta r_4$ (kΩ)
(a)	62.68	−3.0,−7.0	162.6,10.7	3379.6,600.7	675.5,51.3
(b)	69.08	−26.8,11.6	152.9,4.72	3361.7,575.9	654.4,7.7
(c)	62.68	19.8,11.6	189.5,4.72	3398.1,575.9	692.2,7.7
(d)	60.78	9.3,−7.5	173.1,12.5	3390.5,600.9	687.0,52.0

original resistance matrix that involve both r_2 and r_2', i.e., the elements $(R_{12}^{23}, R_{12}^{24}, R_{23}^{12}, R_{24}^{12})$, we were able to fit the non-Ohmic part of the four contact resistances $(\Delta r_i, i=1,4)$. The results are shown in row (b) of Table XI. There is rather good agreement between the two methods, with only a 10% difference in the resistivity. This agreement obtains in spite of the very large and non-Ohmic contact resistance r_3, which dominates the least-squares fitting procedure for the diagonal elements. In general, it is probably best to determine the resistivity from the four-terminal measurements, and so as a final check we used the value of ρ determined from the four-terminal measurements, and did a least-squares fit to obtain the Ohmic part of the contact resistances $(\bar{r}_i, i=1,4)$, from the six diagonal elements of $\bar{R}_{ij}^{lm}$. The non-Ohmic parts of the contact resistance are unchanged by this alternative method of determining the resistivity. These results are shown in row (c) of Table XI. Finally the row (d) of Table XI was given by fitting all parameters by using the whole table.

In this analysis, we noticed that there are some possibilities of error in modeling and fitting as well as experimental measurements. First of all, we suspect the effective contact area in the sample is less than that apparent in the SEM photographs. Some part of the contact might not form good electrical contact with the sample, and hence decreases the real contact area. The sensitivity of diagonal and four-terminal terms has been tested by calculating the resistance changes by shrinking the area of all the contacts by 1/3. The two-terminal measurements varies by, 30–40 % but the four-terminal ones were changed by less than 10%. The resistivity fitted by four-terminal elements turned out more stable than the contact resistances included in two-terminal terms under this change of the contact geometry. Hence the resistivity should be fitted from the four-terminal resistance measurements which are contact-*independent* resistances and the contacts are then obtained subsequently by fitting the whole resistance table. We note that a fine meshing is necessary for reliable results for the geometrical factors for the two-terminal measurements, but a coarser meshing is sufficient to get reliable geometric factors for the four-terminal measurements. And we could get better results by doing the measurements on many different samples that have the same resistivity and with many contacts that give more terms for consistency checks.

Throughout our theoretical treatment, even though we have taken into account the spatial distribution of currents within the sample, there has been no attempt to consider the charge redistribution at surfaces and interfaces, for example, due to band bending. Contact resistances, in particular, will depend on local electric fields which, in turn, will depend on details of the semiconductor-metal interface. In retrospect, it is somewhat surprising that a model invoking local contact resistances should work so well, with contact pad dimensions and separations approaching a space charge depth. If the scale of the experiments were to shrink further, these considerations will need to be treated with more rigor.

V. CONCLUSIONS

A method to measure the resistivity and contact resistances of arbitrarily shaped single crystals has been introduced and demonstrated on micrometer-sized diamond crystallites. The method is quite general, provided that the material of the sample is homogeneous and Ohmic, with contacts that can be non-Ohmic, but should be equipotential surfaces. The sample resistivity and contact resistances were obtained experimentally using four-probe measurements, aided by finite element calculations. This technique can be applied to determine the sample resistivity using any shape of sample. It is possible to determine sample resistivity and the Ohmic part of the contact resistances solely from the set of two-terminal measurements, with currents in both directions, but it is probably best to use the four-terminal measurements to determine the resistivity, and the most accurate results will be obtained from a complete set of resistance measurements with currents in both directions.

ACKNOWLEDGMENTS

We should like to thank J. Bass and W. Pratt Jr. for useful discussions and the NSF Center for Sensor Materials for support. One of us [A.R.D.] would like to thank the Physics Department at Michigan State University for its frequent hospitality.

APPENDIX: RECIPROCITY THEOREM

A sample can be represented by an equivalent circuit of resistors as shown in Fig. 2. We use Kirchhoff's laws to prove the reciprocity theorem using this equivalent circuit. There are d-independent current loops of three resistors in the sample

$$d = r - (n-1) = r - n + 1, \tag{A1}$$

where $r = {}^nC_2$ is a number of resistors and n is a number of vertices. Because there are r unknown currents, $i_1, i_2, \ldots i_r$ on each resistor, we have $n-1$ constraints for currents at each vertex by Kirchhoff's first law of current conservation. Although there are n vertices for constraints, the two constraints on vertices that the external current flows in and out are really a single constraint. Since r is equal to $n(n-1)/2$, the number of independent loops in the circuit is given by

$$d = \frac{n(n-1)}{2} - (n-1) = \frac{(n-1)(n-2)}{2}, \tag{A2}$$

which is one for three leads, three for four leads, six for five leads, and so on. We also have one more loop by the external current i_0 as well as d loops in the sample. We need to set up $d+1$ current loops for Kirchhoff's laws, which give $d+1$ current equations. There is one condition in setting up these loops that each resistor should be included in at least one current loop. To prove the reciprocity theorem, a resistor R_{pq} is selected for external current flow and R_{mn} for voltage measurement. A voltage V is applied across R_{pq} and the current i_0 flows in. Suppose R_{mn} is shared by m current loops $(i_{j+1}, \ldots, i_{j+m})$ and R_{pq} is shared by p current loops $(i_{k+1}, \ldots, i_{k+p})$ and the external current i_0. Now we have $(d+1)$ linear equations from Kirchhoff's law

$$\begin{pmatrix} R_{pq} & 0 & \cdot & 0 & 0 & \cdot & -R_{pq} & -R_{pq} & \cdot & 0 \\ 0 & M_{1,1} & \cdot & \cdot & \cdot & \cdot & \cdot & \cdot & \cdot & \cdot \\ \cdot & \cdot & \cdot & \cdot & \cdot & \cdot & \cdot & \cdot & \cdot & \cdot \\ 0 & \cdot & \cdot & M_{j+1,j+1} & \cdot & \cdot & \cdot & \cdot & \cdot & \cdot \\ 0 & \cdot & \cdot & \cdot & M_{j+m,j+m} & \cdot & M_{j+m,k+1} & \cdot & \cdot & \cdot \\ \cdot & \cdot & \cdot & \cdot & \cdot & \cdot & \cdot & \cdot & \cdot & \cdot \\ -R_{pq} & \cdot & \cdot & \cdot & M_{k+1,j+m} & \cdot & M_{k+1,k+1} & \cdot & \cdot & \cdot \\ -R_{pq} & \cdot & \cdot & \cdot & \cdot & \cdot & \cdot & M_{k+p,k+p} & \cdot & \cdot \\ \cdot & \cdot & \cdot & \cdot & \cdot & \cdot & \cdot & \cdot & \cdot & \cdot \\ 0 & \cdot & \cdot & \cdot & \cdot & \cdot & \cdot & \cdot & \cdot & M_{d,d} \end{pmatrix} \begin{pmatrix} i_0 \\ i_1 \\ \cdot \\ i_{j+1} \\ i_{j+m} \\ \cdot \\ i_{k+1} \\ i_{k+p} \\ \cdot \\ i_d \end{pmatrix} = \begin{pmatrix} V \\ 0 \\ \cdot \\ 0 \\ 0 \\ \cdot \\ 0 \\ 0 \\ \cdot \\ 0 \end{pmatrix} \quad \text{(A3)}$$

where $M_{0,0}$ is R_{pq} and p terms $(M_{0,k+1},\ldots,M_{0,k+p})$ in the 0th column are $-R_{pq}$. In Eq. (A3), $M_{i,j}$ is a matrix element that represents a sum of resistors where the current i_j flows in the ith loop. It is equal to $M_{j,i}$ because those two terms represent the same resistors that are shared by the ith and jth current loops. A solution for i_j from Eq. (A3) is given by

$$i_j = V\,\frac{\Delta_{0,j}}{\Delta}, \quad \text{(A4)}$$

where Δ denotes the determinant of the matrix and $\Delta_{i,j}$ is a cofactor of $M_{i,j}$. Since the net current flow $\Sigma_{a=1}^{m} i_{j+a}$ in R_{mn} is given by the sum of all currents of loops pass through it, a resistance defined by a voltage across m,n and a current through p,q is given by

$$R_{pq}^{mn} = \frac{V_{mn}}{i_0} = \frac{R_{mn}\Sigma_{a=1}^{m} i_{j+a}}{V\,\dfrac{\Delta_{0,0}}{\Delta}} = \frac{R_{mn}\Sigma_{a=1}^{m}\Delta_{0,j+a}}{\Delta_{0,0}}. \quad \text{(A5)}$$

In Eq. (A5), $\Delta_{0,j+a}$ is equal to $-R_{pq}\Sigma_{a=1}^{p}\Delta_{(0,k+b),0,j+a}$ [$\Delta_{(0,k),(0,j)}$, is the determinant of the matrix without the 0th and kth rows and the 0th and jth columns.] because there are p terms of $-R_{pq}$ in the 0th column and the other terms are zero except 0th element R_{pq} irrelevant in calculating $\Delta_{0,j+a}$. From this relation, we have

$$R_{pq}^{mn} = -\frac{R_{mn}R_{pq}\Sigma_{b=1}^{m}\Sigma_{a=1}^{p}\Delta_{(0,k+a),(0,j+b)}}{\Delta_{0,0}}. \quad \text{(A6)}$$

By switching the leads p,q and m,n [it is equivalent to change $k+a$, $j+b$ in this notation], we have another resistance R_{mn}^{pq} defined by a voltage V applied across R_{mn} instead of R_{pq} and a voltage measured across R_{pq}. Since $\Delta_{(0,k+a),(0,j+b)}$ is equal to $\Delta_{(0,j+b),(0,k+a)}$ due to the symmetry of the matrix, we have a symmetric relation by

$$R_{mn}^{pq} = -\frac{R_{pq}R_{mn}\Sigma_{b=1}^{m}\Sigma_{a=1}^{p}\Delta_{(0,j+b),(0,k+a)}}{\Delta_{0,0}} = R_{pq}^{mn}. \quad \text{(A7)}$$

This *reciprocity theorem*[5] says that the resistance from a voltage across p,q and current through m,n is equal to another resistance from voltage across m,n and current through p,q in an equivalent resistor electrical circuit, and therefore in the sample.

[1] S. Kubo, in *Inverse Problems in Engineering Mechanics*, edited by M. Tanaka and H. D. Bui (Springer-Verlag, Heidelberg, 1993), p. 51.

[2] A preliminary account of this work is given in M. D. Jaeger, S. Hyun, A. R. Day, M. F. Thorpe, and B. Golding, Diamond Relat. Mater. **6**, 325 (1997).

[3] L. J. van der Pauw, Phillips Techn. Rdsch. **20**, 230 (1958).

[4] Y. Sun *et al.*, Rev. Sci. Instrum. **63**, 3752 (1992).

[5] B. I. Bleaney and B. Bleaney, *Electricity and Magnetism* (Oxford University Press, Oxford, 1957), p. 69.

[6] H. H. Sample, W. J. Bruno, S. B. Sample, and E. K. Sichel, J. Appl. Phys. **61**, 1079 (1987).

[7] C. Young *et al.*, *Ray Tracing Creations* (Waite Group Press, Corte Madera, 1994), p. 3.

[8] W. H. Press *et al.*, *Numerical Recipes* (Cambridge University Press, New York, 1992), p. 653.

[9] ANSYS is a registered trademark of SAS IP, Inc.

[10] ABAQUS is the product of Hibbitt, Karlsson, and Sorensen, Inc.

[11] For the labeling scheme chosen the contact resistances r_1' and r_4 do not appear in Table VI. A labeling scheme that involves the cyclic permutations of the four indices (i.e., which replaces I_{14} with I_{41}) would be more useful. The resistance table would contain all eight contact resistances, which could then be determined from a single set of measurements.